



Fairfield University  
DigitalCommons@Fairfield

---

Physics Faculty Publications

Physics Department

---

1-1-2007

## Cascade production in the reactions $\gamma p \rightarrow K+K+(X)$ and $\gamma p \rightarrow K+K+\pi-(X)$

L. Guo

Angela Biselli

Fairfield University, [abiselli@fairfield.edu](mailto:abiselli@fairfield.edu)

Follow this and additional works at: <https://digitalcommons.fairfield.edu/physics-facultypubs>

Copyright American Physical Society Publisher final version available at <http://prc.aps.org/abstract/PRC/v76/i2/e025208>

Peer Reviewed

---

### Repository Citation

Guo, L. and Biselli, Angela, "Cascade production in the reactions  $\gamma p \rightarrow K+K+(X)$  and  $\gamma p \rightarrow K+K+\pi-(X)$ " (2007). *Physics Faculty Publications*. 69.

<https://digitalcommons.fairfield.edu/physics-facultypubs/69>

### Published Citation

L. Guo et al., "Cascade production in the reactions  $\gamma p \rightarrow K+K+(X)$  and  $\gamma p \rightarrow K+K+\pi-(X)$ ", *Physical Review C* 76.2 (2007) DOI: 10.1103/PhysRevC.76.025208

This item has been accepted for inclusion in DigitalCommons@Fairfield by an authorized administrator of DigitalCommons@Fairfield. It is brought to you by DigitalCommons@Fairfield with permission from the rights-holder(s) and is protected by copyright and/or related rights. You are free to use this item in any way that is permitted by the copyright and related rights legislation that applies to your use. For other uses, you need to obtain permission from the rights-holder(s) directly, unless additional rights are indicated by a Creative Commons license in the record and/or on the work itself. For more information, please contact [digitalcommons@fairfield.edu](mailto:digitalcommons@fairfield.edu).

## Cascade production in the reactions $\gamma p \rightarrow K^+ K^+(X)$ and $\gamma p \rightarrow K^+ K^+ \pi^-(X)$

L. Guo,<sup>1,\*</sup> D. P. Weygand,<sup>1</sup> M. Battaglieri,<sup>2</sup> R. De Vita,<sup>2</sup> V. Kubarovsky,<sup>3</sup> P. Stoler,<sup>3</sup> M. J. Amarian,<sup>30</sup> P. Ambrozewicz,<sup>15</sup> M. Anghinolfi,<sup>2</sup> G. Asryan,<sup>39</sup> H. Avakian,<sup>1</sup> H. Bagdasaryan,<sup>30</sup> N. Baillie,<sup>38</sup> J. P. Ball,<sup>5</sup> N. A. Baltzell,<sup>33</sup> V. Batourine,<sup>24</sup> M. Battaglieri,<sup>2</sup> I. Bedlinskiy,<sup>22</sup> M. Bellis,<sup>3,8</sup> N. Benmouna,<sup>17</sup> B. L. Berman,<sup>17</sup> A. S. Biselli,<sup>8,14</sup> L. Blaszczyk,<sup>16</sup> S. Bouchigny,<sup>21</sup> S. Boiarinov,<sup>1</sup> R. Bradford,<sup>8</sup> D. Branford,<sup>13</sup> W. J. Briscoe,<sup>17</sup> W. K. Brooks,<sup>1</sup> S. Bültmann,<sup>30</sup> V. D. Burkert,<sup>1</sup> C. Butuceanu,<sup>38</sup> J. R. Calarco,<sup>27</sup> S. L. Careccia,<sup>30</sup> D. S. Carman,<sup>1</sup> S. Chen,<sup>16</sup> P. L. Cole,<sup>19</sup> P. Collins,<sup>5</sup> P. Coltharp,<sup>16</sup> D. Crabb,<sup>37</sup> H. Crannell,<sup>9</sup> V. Crede,<sup>16</sup> J. P. Cummings,<sup>3</sup> N. Dashyan,<sup>39</sup> R. De Masi,<sup>10</sup> R. De Vita,<sup>2</sup> E. De Sanctis,<sup>20</sup> P. V. Degtyarenko,<sup>1</sup> A. Deur,<sup>1</sup> K. V. Dharmawardane,<sup>30</sup> R. Dickson,<sup>8</sup> C. Djalali,<sup>33</sup> G. E. Dodge,<sup>30</sup> J. Donnelly,<sup>18</sup> D. Doughty,<sup>1,11</sup> M. Dugger,<sup>5</sup> O. P. Dzyubak,<sup>33</sup> H. Egiyan,<sup>1,†</sup> K. S. Egiyan,<sup>39</sup> L. El Fassi,<sup>4</sup> L. Elouadrhiri,<sup>1</sup> P. Eugenio,<sup>16</sup> G. Fedotov,<sup>26</sup> G. Feldman,<sup>17</sup> H. Funsten,<sup>38</sup> M. Garçon,<sup>10</sup> G. Gavalian,<sup>27,30</sup> G. P. Gilfoyle,<sup>32</sup> K. L. Giovanetti,<sup>23</sup> F. X. Girod,<sup>10</sup> J. T. Goetz,<sup>6</sup> A. Gonenc,<sup>15</sup> C. I. O. Gordon,<sup>18</sup> R. W. Gothe,<sup>33</sup> K. A. Griffioen,<sup>38</sup> M. Guidal,<sup>21</sup> N. Guler,<sup>30</sup> V. Gyurjyan,<sup>1</sup> C. Hadjidakis,<sup>21</sup> K. Hafidi,<sup>4</sup> H. Hakobyan,<sup>39</sup> R. S. Hakobyan,<sup>9</sup> C. Hanretty,<sup>16</sup> J. Hardie,<sup>1,11</sup> F. W. Hersman,<sup>27</sup> K. Hicks,<sup>29</sup> I. Hleiqawi,<sup>29</sup> M. Holtrop,<sup>27</sup> C. E. Hyde-Wright,<sup>30</sup> Y. Ilieva,<sup>17</sup> D. G. Ireland,<sup>18</sup> B. S. Ishkhanov,<sup>26</sup> E. L. Isupov,<sup>26</sup> M. M. Ito,<sup>1</sup> D. Jenkins,<sup>36</sup> R. Johnstone,<sup>18</sup> H. S. Jo,<sup>21</sup> K. Joo,<sup>12</sup> H. G. Juengst,<sup>17,30</sup> N. Kalantarians,<sup>30</sup> J. D. Kellie,<sup>18</sup> M. Khandaker,<sup>28</sup> W. Kim,<sup>24</sup> A. Klein,<sup>30</sup> F. J. Klein,<sup>9</sup> A. V. Klimenko,<sup>30</sup> M. Kossov,<sup>22</sup> Z. Krahn,<sup>8</sup> L. H. Kramer,<sup>1,15</sup> J. Kuhn,<sup>8</sup> S. E. Kuhn,<sup>30</sup> S. V. Kuleshov,<sup>22</sup> J. Lachniet,<sup>8,30</sup> J. M. Laget,<sup>1,10</sup> J. Langheinrich,<sup>33</sup> D. Lawrence,<sup>25</sup> T. Lee,<sup>27</sup> Ji Li,<sup>3</sup> K. Livingston,<sup>18</sup> H. Y. Lu,<sup>33</sup> M. MacCormick,<sup>21</sup> N. Markov,<sup>12</sup> P. Mattione,<sup>31</sup> B. McKinnon,<sup>18</sup> B. A. Mecking,<sup>1</sup> J. J. Melone,<sup>18</sup> M. D. Mestayer,<sup>1</sup> C. A. Meyer,<sup>8</sup> T. Mibe,<sup>29</sup> K. Mikhailov,<sup>22</sup> R. Minehart,<sup>37</sup> M. Mirazita,<sup>20</sup> R. Miskimen,<sup>25</sup> V. Mokeev,<sup>26</sup> K. Moriya,<sup>8</sup> S. A. Morrow,<sup>10,21</sup> M. Moteabbed,<sup>15</sup> E. Munevar,<sup>17</sup> G. S. Mutchler,<sup>31</sup> P. Nadel-Turonski,<sup>17</sup> R. Nasseripour,<sup>15,33</sup> S. Niccolai,<sup>21</sup> G. Niculescu,<sup>23</sup> I. Niculescu,<sup>23</sup> B. B. Niczyporuk,<sup>1</sup> M. R. Niroula,<sup>30</sup> R. A. Niyazov,<sup>1</sup> M. Nozar,<sup>1,34</sup> M. Osipenko,<sup>2,26</sup> A. I. Ostrovidov,<sup>16</sup> K. Park,<sup>24</sup> E. Pasyuk,<sup>5</sup> C. Paterson,<sup>18</sup> S. Anefalos Pereira,<sup>20</sup> J. Pierce,<sup>37</sup> N. Pivnyuk,<sup>22</sup> D. Pocanic,<sup>37</sup> O. Pogorelko,<sup>22</sup> S. Pozdniakov,<sup>22</sup> J. W. Price,<sup>7</sup> Y. Prok,<sup>37,‡</sup> D. Protopopescu,<sup>18</sup> B. A. Raue,<sup>1,15</sup> G. Riccardi,<sup>16</sup> G. Ricco,<sup>2</sup> M. Ripani,<sup>2</sup> B. G. Ritchie,<sup>5</sup> F. Ronchetti,<sup>20</sup> G. Rosner,<sup>18</sup> P. Rossi,<sup>20</sup> F. Sabatié,<sup>10</sup> J. Salamanca,<sup>19</sup> C. Salgado,<sup>28</sup> J. P. Santoro,<sup>1,36,§</sup> V. Sapunenko,<sup>1</sup> R. A. Schumacher,<sup>8</sup> V. S. Serov,<sup>22</sup> Y. G. Sharabian,<sup>1</sup> D. Sharov,<sup>26</sup> N. V. Shvedunov,<sup>26</sup> E. S. Smith,<sup>1</sup> L. C. Smith,<sup>37</sup> D. I. Sober,<sup>9</sup> D. Sokhan,<sup>13</sup> A. Stavinsky,<sup>22</sup> S. S. Stepanyan,<sup>24</sup> S. Stepanyan,<sup>1</sup> B. E. Stokes,<sup>16</sup> I. I. Strakovsky,<sup>17</sup> S. Strauch,<sup>17,33</sup> M. Taiuti,<sup>2</sup> D. J. Tedeschi,<sup>33</sup> U. Thoma,<sup>1,||</sup> A. Tkabladze,<sup>17,29</sup> S. Tkachenko,<sup>30</sup> L. Todor,<sup>32</sup> C. Tur,<sup>33</sup> M. Ungaro,<sup>3,12</sup> M. F. Vineyard,<sup>35</sup> A. V. Vlassov,<sup>22</sup> D. P. Watts,<sup>18,¶</sup> L. B. Weinstein,<sup>30</sup> M. Williams,<sup>8</sup> E. Wolin,<sup>1</sup> M. H. Wood,<sup>33,\*</sup> A. Yegneswaran,<sup>1</sup> L. Zana,<sup>27</sup> J. Zhang,<sup>30</sup> B. Zhao,<sup>12</sup> and Z. W. Zhao<sup>33</sup>

(CLAS Collaboration)

<sup>1</sup>Thomas Jefferson National Accelerator Facility, Newport News, Virginia 23606, USA<sup>2</sup>INFN, Sezione di Genova, 16146 Genova, Italy<sup>3</sup>Rensselaer Polytechnic Institute, Troy, New York 12180-3590, USA<sup>4</sup>Argonne National Laboratory, Argonne, Illinois 60439, USA<sup>5</sup>Arizona State University, Tempe, Arizona 85287-1504, USA<sup>6</sup>University of California at Los Angeles, Los Angeles, California 90095-1547, USA<sup>7</sup>California State University, Dominguez Hills, Carson, California 90747, USA<sup>8</sup>Carnegie Mellon University, Pittsburgh, Pennsylvania 15213, USA<sup>9</sup>Catholic University of America, Washington, DC 20064, USA<sup>10</sup>CEA-Saclay, Service de Physique Nucléaire, F-91191 Gif-sur-Yvette, France<sup>11</sup>Christopher Newport University, Newport News, Virginia 23606, USA<sup>12</sup>University of Connecticut, Storrs, Connecticut 06269, USA<sup>13</sup>Edinburgh University, Edinburgh EH9 3JZ, United Kingdom<sup>14</sup>Fairfield University, Fairfield, Connecticut 06824, USA<sup>15</sup>Florida International University, Miami, Florida 33199, USA<sup>16</sup>Florida State University, Tallahassee, Florida 32306, USA<sup>17</sup>The George Washington University, Washington, DC 20052, USA<sup>18</sup>University of Glasgow, Glasgow G12 8QQ, United Kingdom<sup>19</sup>Idaho State University, Pocatello, Idaho 83209, USA<sup>20</sup>INFN, Laboratori Nazionali di Frascati, I-00044 Frascati, Italy<sup>21</sup>Institut de Physique Nucleaire ORSAY, Orsay, France<sup>22</sup>Institute of Theoretical and Experimental Physics, RU-117259 Moscow, Russia<sup>23</sup>James Madison University, Harrisonburg, Virginia 22807, USA<sup>24</sup>Kyungpook National University, Daegu 702-701, South Korea<sup>25</sup>University of Massachusetts, Amherst, Massachusetts 01003, USA<sup>26</sup>Moscow State University, Skobeltsyn Nuclear Physics Institute, RU-119899 Moscow, Russia<sup>27</sup>University of New Hampshire, Durham, New Hampshire 03824-3568, USA<sup>28</sup>Norfolk State University, Norfolk, Virginia 23504, USA<sup>29</sup>Ohio University, Athens, Ohio 45701, USA

<sup>30</sup>*Old Dominion University, Norfolk, Virginia 23529, USA*<sup>31</sup>*Rice University, Houston, Texas 77005-1892, USA*<sup>32</sup>*University of Richmond, Richmond, Virginia 23173, USA*<sup>33</sup>*University of South Carolina, Columbia, South Carolina 29208, USA*<sup>34</sup>*TRIUMF, Vancouver, British Columbia V6T 2A3, Canada*<sup>35</sup>*Union College, Schenectady, New York 12308, USA*<sup>36</sup>*Virginia Polytechnic Institute and State University, Blacksburg, Virginia 24061-0435, USA*<sup>37</sup>*University of Virginia, Charlottesville, Virginia 22901, USA*<sup>38</sup>*College of William and Mary, Williamsburg, Virginia 23187-8795, USA*<sup>39</sup>*Yerevan Physics Institute, 375036 Yerevan, Armenia*

(Received 8 March 2007; published 14 August 2007)

Photoproduction of the cascade resonances has been investigated in the reactions  $\gamma p \rightarrow K^+ K^+(X)$  and  $\gamma p \rightarrow K^+ K^+ \pi^-(X)$ . The mass splitting of the ground state ( $\Xi^-, \Xi^0$ ) doublet is measured to be  $5.4 \pm 1.8$  MeV/ $c^2$ , consistent with existing measurements. The differential (total) cross sections for the  $\Xi^-$  have been determined for photon beam energies from 2.75 to 3.85 (4.75) GeV and are consistent with a production mechanism of  $Y^* \rightarrow K^+ \Xi^-$  through a  $t$ -channel process. The reaction  $\gamma p \rightarrow K^+ K^+ \pi^- [\Xi^0]$  has also been investigated to search of excited cascade resonances. No significant signal of excited cascade states other than the  $\Xi^-(1530)$  is observed. The cross-section results of the  $\Xi^-(1530)$  have also been obtained for photon beam energies from 3.35 to 4.75 GeV.

DOI: [10.1103/PhysRevC.76.025208](https://doi.org/10.1103/PhysRevC.76.025208)

PACS number(s): 13.60.Rj, 12.40.Yx, 14.20.Jn, 25.20.Lj

## I. INTRODUCTION

Hadron spectroscopy is an essential experimental means of accessing fundamental parameters of QCD such as quark masses. The average of the baryon ground-state isospin multiplet ( $N, \Sigma, \Delta, \Xi, \Sigma_c, \Xi_c$ ) mass differences yields a value of  $m_d - m_u = +(2.8 \pm 0.3)$  MeV/ $c^2$  [1], with the  $\Xi$  ground-state doublet being the most intriguing.

The current global measurement of the mass difference between the  $\Xi^0(uss)$  and  $\Xi^-(dss)$  is  $6.48 \pm 0.24$  MeV/ $c^2$  according to the PDG [2], considerably larger than that of the other multiplets. A calculation on the QCD lattice [3] gives a result of  $5.68 \pm 0.24$  MeV/ $c^2$ , whereas a calculation based on radiative corrections to the quark model [4] gives  $6.10$  MeV/ $c^2$ . Experimentally, however, only one measurement of the  $\Xi^0$  mass has more than 50 events [5].

Compared with nonstrange baryons and  $S = -1$  hyperon states, the  $\Xi$  resonances are generally underexplored. Only two ground-state cascades, the octet member  $\Xi$  and the decuplet member  $\Xi(1530)$ , have four-star status in the PDG [2], with four other three-star candidates. The lack of data is mainly due

to smaller  $\Xi^{(*)}$  cross sections than the  $S = 0$  and  $-1$  baryons and the fact that cascade resonances cannot be produced through direct formation. More than 20  $N^*$  and  $\Delta^*$  resonances are rated with at least three stars in the PDG [2]. Flavor SU(3) symmetry predicts as many  $\Xi$  resonances as  $N^*$  and  $\Delta^*$  states combined, suggesting that many more cascade resonances remain undiscovered. Of the six  $\Xi$  states that have at least three-star ratings in the PDG, only three have spin-parity ( $J^P$ ) determined:  $\Xi(1320)_{\frac{1}{2}}^+$ ,  $\Xi(1530)_{\frac{3}{2}}^+$ , and  $\Xi(1820)_{\frac{3}{2}}^-$ .

In general, the production mechanisms of the cascade resonances remain unclear. Kaon and hyperon beam experiments conducted to investigate cascade spectroscopy suffer from either low intensity or high combinatorial background. Results from earlier kaon beam experiments indicate that it is possible to produce the  $\Xi$  ground state through the decay of high-mass  $Y^*$  states [6–9]. It is therefore possible to produce cascade resonances through  $t$ -channel photoproduction of hyperon resonances as indicated in Fig. 1.

By using tagged photons incident on a proton target, it has been demonstrated that cascade production can be investigated through exclusive reactions, such as  $\gamma p \rightarrow K^+ K^+(X)$  [10] in CLAS. Prior to this publication, only two groups have reported measurements of cascade photoproduction, both in the inclusive reaction  $\gamma p \rightarrow \Xi^- X$  by reconstructing the  $\Xi^-$  from the decay  $\Xi^- \rightarrow \Lambda \pi^- \rightarrow p \pi^- \pi^-$ . The CERN SPS experiment with the Omega spectrometer [11] measured a cross section of  $28 \pm 9$  nb for the kinematical range  $x_F (= 2p_{\parallel}^*/\sqrt{s}) > -0.3$ , using a tagged photon beam in the energy range 20–70 GeV. However, the SLAC 1-m hydrogen bubble chamber experiment [12] using a 20-GeV photon beam reported a much higher cross section of  $94 \pm 13$  nb in the same  $x_F$  range, with a total cross section of  $117 \pm 17$  nb.

The SLAC results showed that the  $x_F$  distribution of the  $\Xi^-$  events peaks around  $-\frac{1}{3}$ , consistent with a quark-diquark fusion production mechanism [13], in which the cascade has

\*Corresponding author: lguo@jlab.org

†Current address: University of New Hampshire, Durham, New Hampshire 03824-3568, USA.

‡Current address: Massachusetts Institute of Technology, Cambridge, Massachusetts 02139-4307, USA.

§Current address: Catholic University of America, Washington, DC 20064, USA.

||Current address: Physikalisches Institut der Universitaet Giessen, D-35392 Giessen, Germany.

¶Current address: Edinburgh University, Edinburgh EH9 3JZ, United Kingdom.

\*\*Current address: University of Massachusetts, Amherst, Massachusetts 01003, USA.

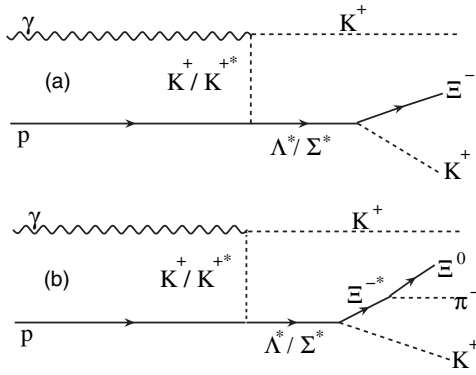


FIG. 1. Possible photoproduction mechanisms of  $\Xi$  ground states through intermediate hyperon resonances produced in a  $t$ -channel process: (a)  $\Xi^-$  production; (b)  $\Xi^0$  production.

one out of three quarks in common with the proton. However, such a model is more appropriate for inclusive reactions at high energies where partonic degrees of freedom are more relevant, and it is not applicable for exclusive reactions at low to intermediate energies compared with the threshold ( $E_\gamma^{\text{thres}} = 2.37$  GeV). Recently, Nakayama *et al.* [14] developed a  $\Xi$  production model for the exclusive reaction  $\gamma N \rightarrow K K \Xi$  from an effective Lagrangian that incorporates various  $t$ -,  $u$ -, and  $s$ -channel processes, taking into account intermediate hyperon and nucleon resonances. (Details of the model will be discussed later in this paper.) The validity of the model should be checked by comparing its predictions with experimental data.

In this paper, the mass difference of the  $\Xi$  doublet and the cross sections of the  $\Xi^-$  and  $\Xi^-(1530)$  are reported and compared with the results of Ref. [14]. The possibility of producing other excited cascade states in photon-proton reactions is also discussed.

## II. EXPERIMENT

A new large-statistics data set, with an integrated luminosity of  $70 \text{ pb}^{-1}$ , was collected at CLAS [15] from May to July 2004 by using a tagged photon beam [16] incident on a proton target. This data set is mostly in the energy range of 1.6–3.85 GeV with a primary electron beam energy ( $E_0$ ) of 4 GeV. About 5% of the data were collected with  $E_0 = 5$  GeV. The target consists of a 40-cm-long cylindrical cell containing liquid hydrogen. Momentum information for charged particles was obtained via tracking through three regions of multiwire drift chambers [17] inside a toroidal magnetic field ( $\sim 0.5$  T), generated by six superconducting coils. Time-of-flight (TOF) scintillators were used for charged hadron identification [18]. The interaction time between the incoming photon and the target was measured by the start counter [19], consisting of 24 strips of 2.2-mm-thick plastic scintillators surrounding the target cell. Coincidences between the photon tagger and two charged particles in the CLAS detector triggered the events.

Cascade states can be identified via missing mass, through the reaction  $\gamma p \rightarrow K^+ K^+(X)$ , or via the decay  $\Xi^{*-} \rightarrow \Xi^0 \pi^-$  through the reaction  $\gamma p \rightarrow K^+ K^+ \pi^-(X)$ . In the reaction

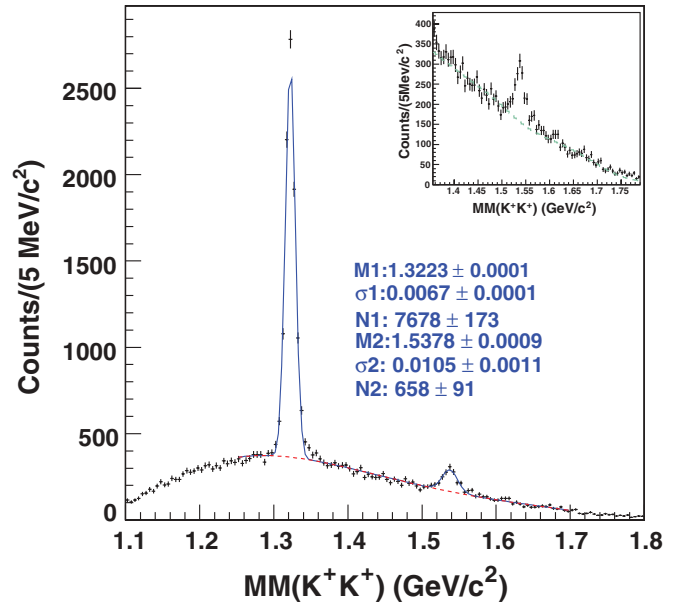


FIG. 2. (Color online)  $MM(K^+K^+)$  distribution for  $E_\gamma > 2.6$  GeV fitted with two Gaussian functions and an empirical background shape with adjustable normalization (M: mean of the Gaussian peak position,  $\sigma$ : width of the Gaussian signal, N: number of events in the peak) (Inset)  $MM(K^+K^+)$  distribution enlarged for the 1.36–1.79  $\text{GeV}/c^2$  region, the dashed lines show the empirical background shape from  $K^-$  events normalized to the region of 1.36–1.5  $\text{GeV}/c^2$ .

$\gamma p \rightarrow K^+ K^+(X)$ , the double strangeness is tagged by the two positive kaons detected by CLAS, and the cascade resonances are observed in the  $K^+ K^+$  missing-mass spectrum (Fig. 2). Without the more stringent particle identification criteria that were applied in Fig. 2 (i.e, the kaon vertex time determined by the TOF is within 1 ns of the photon time given by the RF), more than 12,000  $\Xi^-$ s were observed [20]. After the tighter detector timing cut was applied, about 7700  $\Xi^-$  events are identified for the photon energy range of 2.6–4.75 GeV. There is no  $\Xi^-$  signal for  $E_\gamma < 2.6$  GeV, most likely because of low acceptance.

The  $\Xi^-(1530)$  is clearly present in the spectrum, with about 700 events (Fig. 2). Events with an additional  $K^-$  detected are used as an empirical background, since the background is dominated by reactions such as  $\gamma p \rightarrow K^+ K^- p$  or  $\gamma p \rightarrow K^+ K^- \pi^+ n$ , with the proton or  $\pi^+$  misidentified as a  $K^+$ . (Potential background processes such as  $\gamma p \rightarrow \phi \Lambda K^+$  were explored and found to be insignificant.) The background is then smoothed and normalized to the region between the  $\Xi^-$  and the  $\Xi^-(1530)$  resonances (1.36–1.5  $\text{GeV}/c^2$ ) in the  $MM(K^+K^+)$  distribution (Fig. 2, inset). The  $\Xi^-$  mass is determined to be  $1322.3 \pm 0.1 \pm 1.2 \text{ MeV}/c^2$ , slightly higher than the PDG [2] value but within errors. The systematic uncertainty is derived from studying the variation of the fitted mass centroid as a function of  $E_\gamma$ . The  $\Xi^-$  width is  $6.7 \pm 0.1 \text{ MeV}/c^2$ , which is consistent with the missing-mass resolution of CLAS as expected from simulation. It is mostly dependent on the resolution of the photon energy measurement, which is typically around 0.1% of the incident photon energy [21].

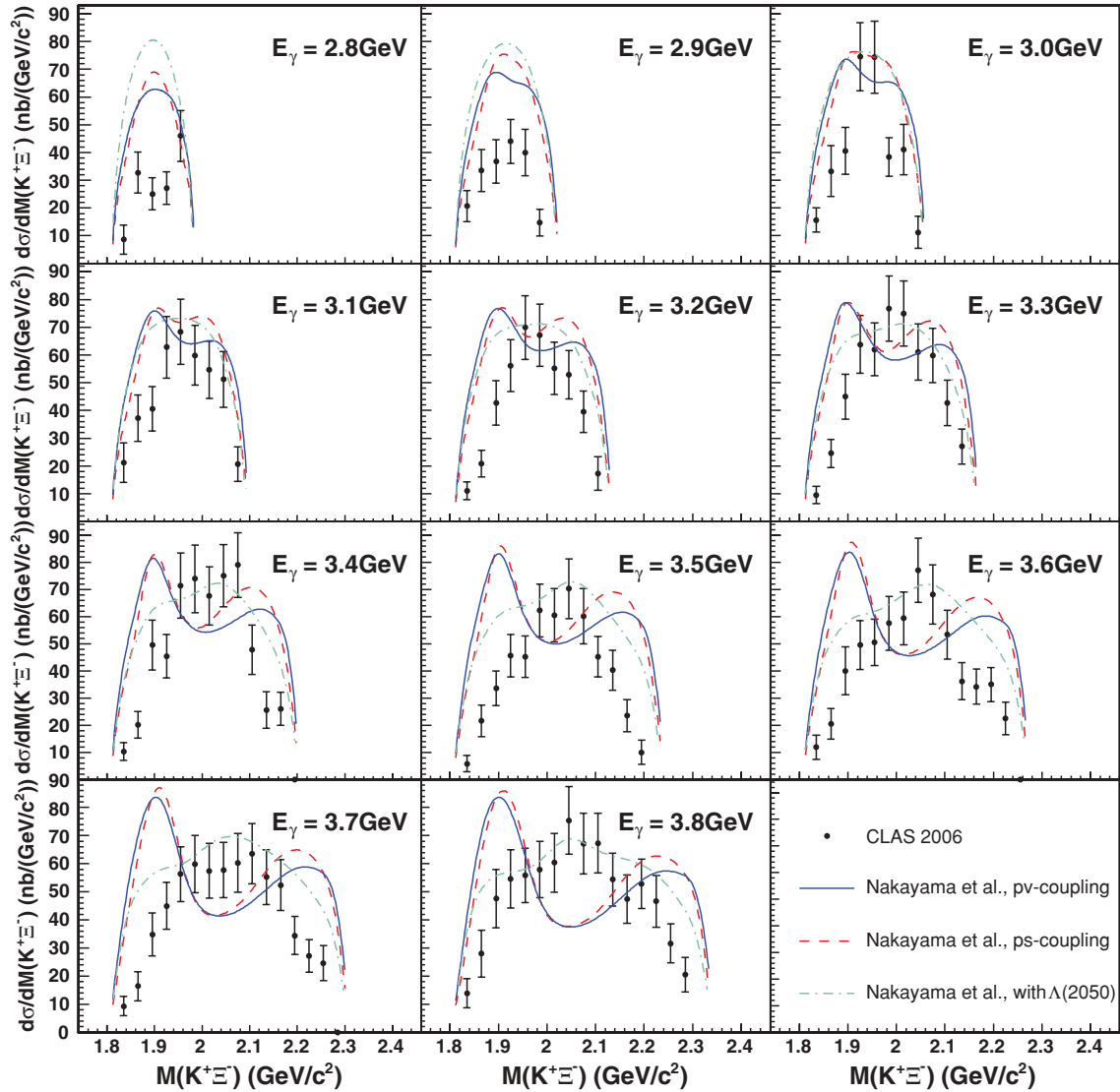


FIG. 3. (Color online) Differential cross section  $[d\sigma/dM(K^+\Xi^-)]$  results (including both statistical and systematic uncertainties) from the current work compared with model predictions from Ref. [14]. The solid curves correspond to the predictions with the  $pv$ -coupling choice, the dashed curves correspond to the  $ps$ -coupling choice, and the dot-dashed curves include an additional  $\frac{3}{2}^+$  hyperon resonance at  $2.05 \text{ GeV}/c^2$  with  $\Gamma = 200 \text{ MeV}/c^2$ .

### III. $\Xi^-$ CROSS-SECTION RESULTS

The observed  $\Xi^-$  events in this work represent the highest statistics seen in exclusive photoproduction to date. It is possible to probe the production mechanism through various differential cross sections, such as  $d\sigma/dM(K^+\Xi^-)$ ,  $d\sigma/dM(K^+K^+)$ ,  $d\sigma/d\cos\theta_{\Xi^-}$ , and  $d\sigma/d\cos\theta_{K^+}$ . To extract the cross section for the  $\Xi^-$ , a detailed simulation has been carried out. Assuming a  $t$ -channel process, we simulated the reaction  $\gamma p \rightarrow K^+Y^*$ ,  $Y^* \rightarrow K^+\Xi^-$ . Although earlier experiments have reported the possible observation of  $Y^* \rightarrow \Xi K$  for the  $\Sigma(2030)(J^P = \frac{7}{2}^+)$  and  $\Lambda(2100)(J^P = \frac{7}{2}^-)$  states [6–9], these results remain questionable because of low statistics, and the results have not been corroborated. Therefore, the parameters of our simulation [ $M(Y^*)$ ,  $\Gamma(Y^*)$ , and exponential  $t$ -slope values] were adjusted

iteratively to match the data distributions. The final parameters for the  $Y^*$  are  $M = 1.96 \text{ GeV}/c^2$  and  $\Gamma = 220 \text{ MeV}/c^2$ . The  $t$ -slope values range from 1.11 to 2.64  $(\text{GeV}/c^2)^{-2}$  for the 11 photon energy bins from 2.75 to 3.85 GeV. After the simulation successfully reproduced the data, the differential cross section results for the  $\Xi^-$  were then extracted for the photon energy range of 2.75–3.85 GeV. Because of limited statistics, only total cross sections in the photon energy range of 3.85–4.75 GeV have been extracted.

Although the quark-diquark fusion mechanism was used to explain earlier  $\Xi^-$  inclusive photoproduction data, hadronic degrees of freedom are of more relevance at the energy range of this experiment. Partly owing to the lack of data, there have been no theoretical predictions of the cascade production in exclusive photon-nucleon reactions until the production model developed by Nakayama *et al.* [14] for

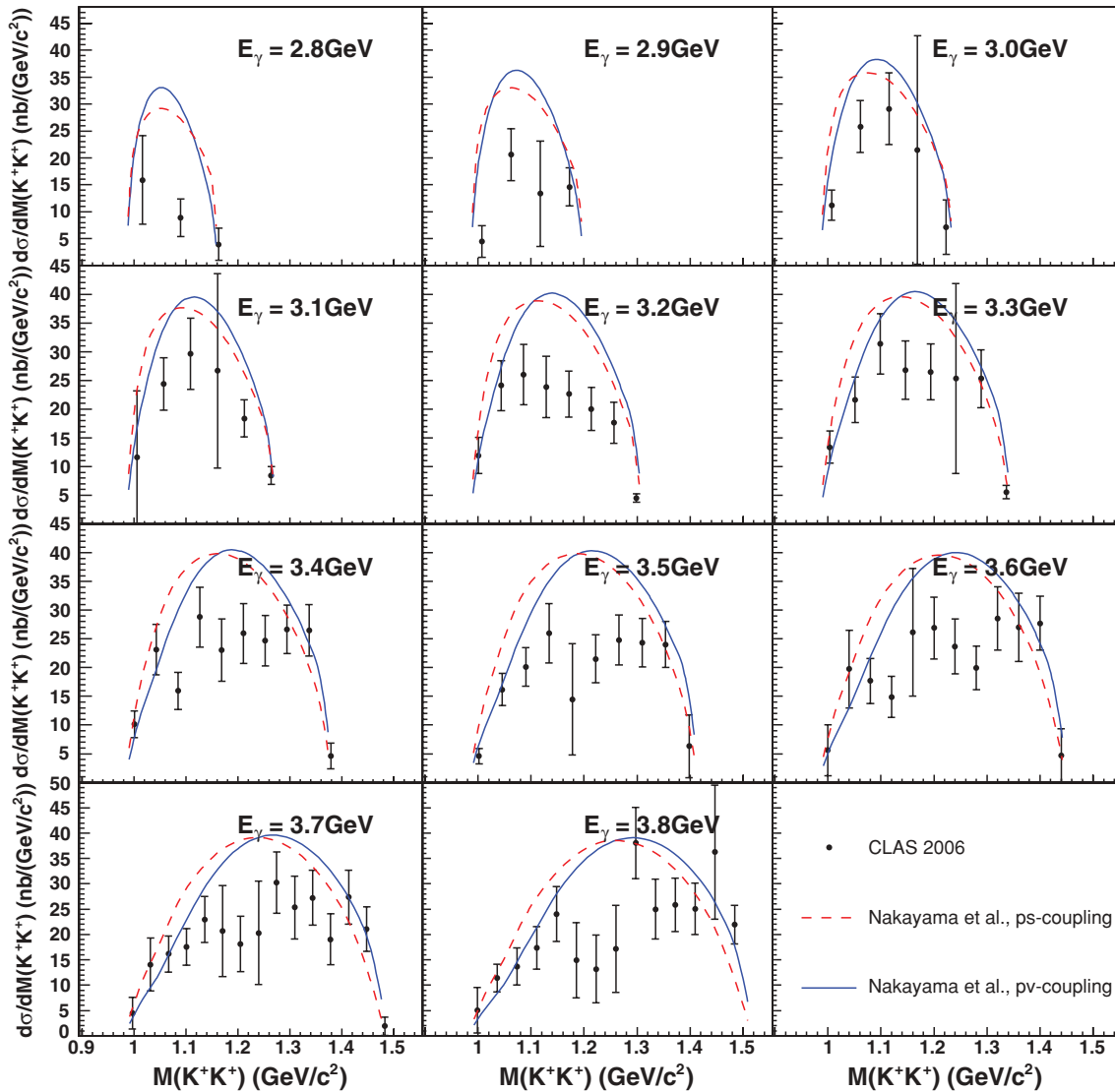


FIG. 4. (Color online) Differential cross section  $[d\sigma/dM(K^+K^+)]$  results (including both statistical and systematic uncertainties) from the current work compared with model predictions from Ref. [14]. The solid curves correspond to the predictions with the pv-coupling choice; the dashed curves correspond to the ps-coupling choice.

the reaction  $\gamma N \rightarrow KK\Xi$ . By using an effective Lagrangian approach, the model incorporates various  $t$ -,  $u$ -, and  $s$ -channel processes, accounting for intermediate hyperon and nucleon resonances. The free parameters include the pseudoscalar-pseudovector (ps-pv) mixing parameter  $\lambda$ , the signs of the hadronic and electromagnetic transition coupling constants, the cutoff parameter  $\Lambda_B$  and the exponent  $n$  in the baryonic form factor  $f_B [f_B(p^2) = (\frac{n\Lambda_B^4}{n\Lambda_B^4 + (p^2 - m_B^2)^2})^n]$ , with  $p$  denoting the baryon momentum and  $m_B$  the baryon mass], and the product of the coupling constants  $g_{N\Lambda K}g_{\Xi\Lambda K}$  for higher mass resonances. In their model, the ps-choice and pv-choice denote the extreme cases for the pseudoscalar-pseudovector (ps-pv) mixing parameter  $\lambda$  (i.e.,  $\lambda = 0$  for the pv-coupling choice and  $\lambda = 1$  for the ps-coupling choice).

Although Ref. [14] includes predictions using many variations of the parameters, the best agreement with our data requires  $t$ -channel processes involving at least one  $J = \frac{3}{2}$

hyperon. Therefore, the more interesting differential cross sections would be  $d\sigma/dM(K^+\Xi^-)$ . Since there are two  $K^+$  in the final state, both particles are included in the differential cross section extractions (Fig. 3). The model of Ref. [14] includes the  $\Lambda(1800)\frac{1}{2}^-$  and the  $\Lambda(1890)\frac{3}{2}^+$ , predicting a double-humped behavior for the  $M(\Xi^-K^+)$  spectra (Fig. 3, solid and dashed curves). However, such a feature could potentially be smoothed out if an additional hypothetical hyperon state [ $\Lambda(2050)\frac{3}{2}^+$ , with  $\Gamma = 200$  MeV/ $c^2$ ] is included in the model. The predictions agree with the data qualitatively when the additional  $\Lambda(2050)$  state is included (Fig. 3, dot-dashed curves).

As for the hyperon states at lower masses, the data do not appear to support significant contributions from the  $\Lambda(1800)$  and the  $\Lambda(1890)$ , since the  $K^+\Xi^-$  invariant mass spectra (Fig. 3) peak significantly higher, at positions shifting according to the the photon energies. Whether these enhancements

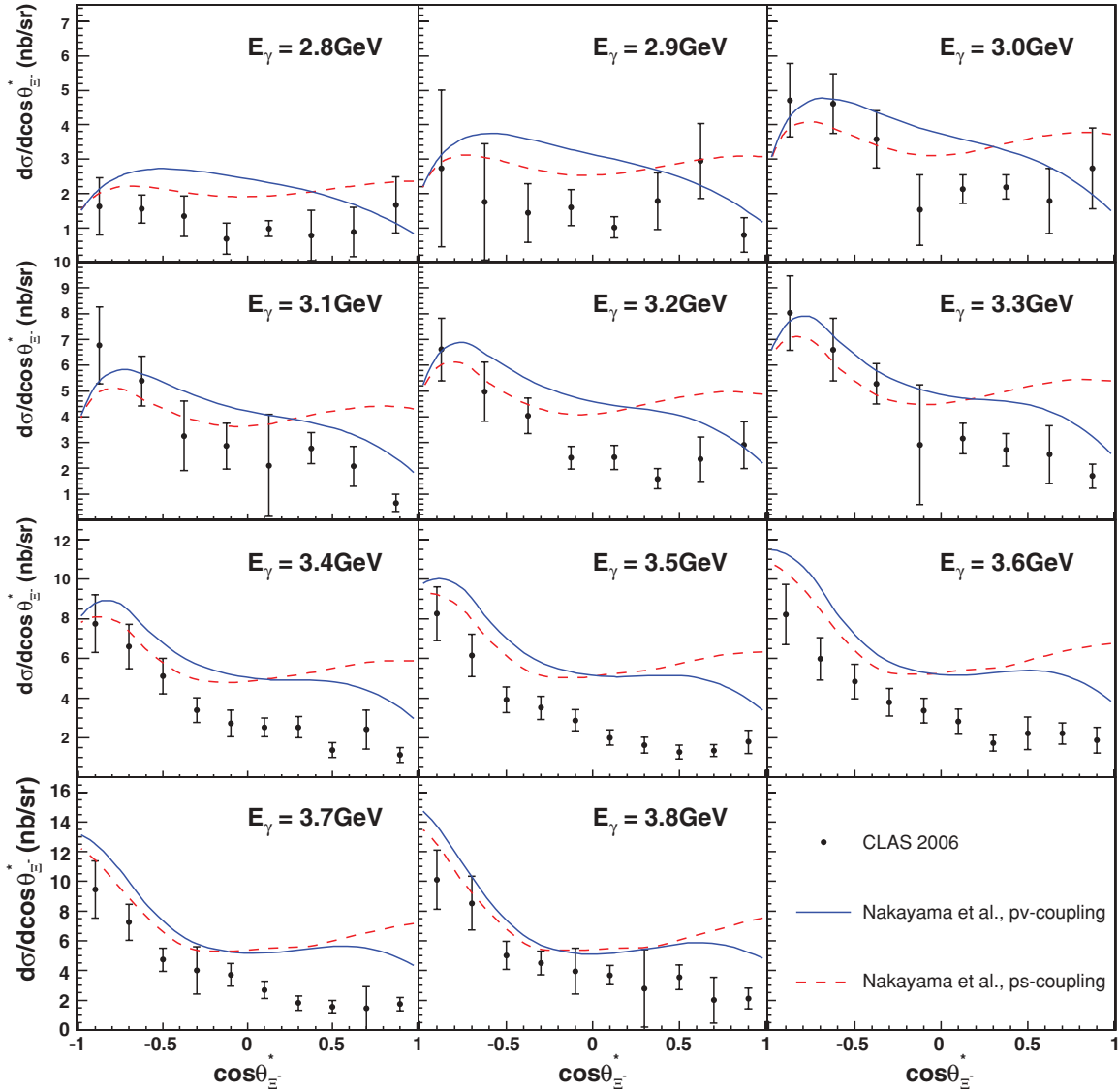


FIG. 5. (Color online) Differential cross section ( $d\sigma/d\cos\theta_{\Xi^-}^*$ ) results (including both statistical and systematic uncertainties) from the current work compared with model predictions from Ref. [14]. The solid curves correspond to the predictions with the pv-coupling choice; the dashed curves correspond to the ps-coupling choice.

are due to hyperon states that decay to  $K^+\Xi^-$  or simply to larger phase space could not be sufficiently determined by the current analysis. Further work by Mokeev *et al.* on the development of the JLAB-MSU phenomenological approach [22] for exclusive reactions with three final state particles to incorporate the  $K^+K^+\Xi^-$  channel is in progress, and their results may help to better determine the  $\Xi^-$  photoproduction mechanism in the future.

Since no  $S = +2$  meson system is believed to contribute to the reaction  $\gamma p \rightarrow K^+K^+\Xi^-$ , the  $K^+K^+$  invariant mass spectrum is expected to be featureless, as is supported by both the data and the model of Nakayama *et al.* [14] (Fig. 4).

The angular distributions of the  $\Xi^-$  and  $K^+$  in the photon-proton center-of-mass (c.m.) frame are also studied (Figs. 5 and 6). In Fig. 5, the  $\Xi^-$  angular distributions in the c.m. frame appear to be peaking backward for most of the energy

bins, qualitatively agreeing with the predictions of Ref. [14], which seems to overestimate the contributions from radiative transitional processes that tend to create forward-peaking features. As for the  $K^+$  c.m. angular distributions (Fig. 6), the data exhibit a somewhat forward-peaking feature although it decreases in the most forward region. These angular distributions are consistent with the predictions that  $\Xi^-$  photoproduction is dominated by  $t$ -channel hyperon processes.

The statistical uncertainties of the differential cross section results are around 15%. Systematic uncertainties from the detector uncertainties, fiducial cuts, and flux normalization factors amount to around 10%. Systematic uncertainties from model dependence of the acceptance is extracted for each kinematic bin by comparing the values obtained using a range of simulation parameters. Such uncertainties are typically less than 5%, but they may be as high as 10% for particular angular

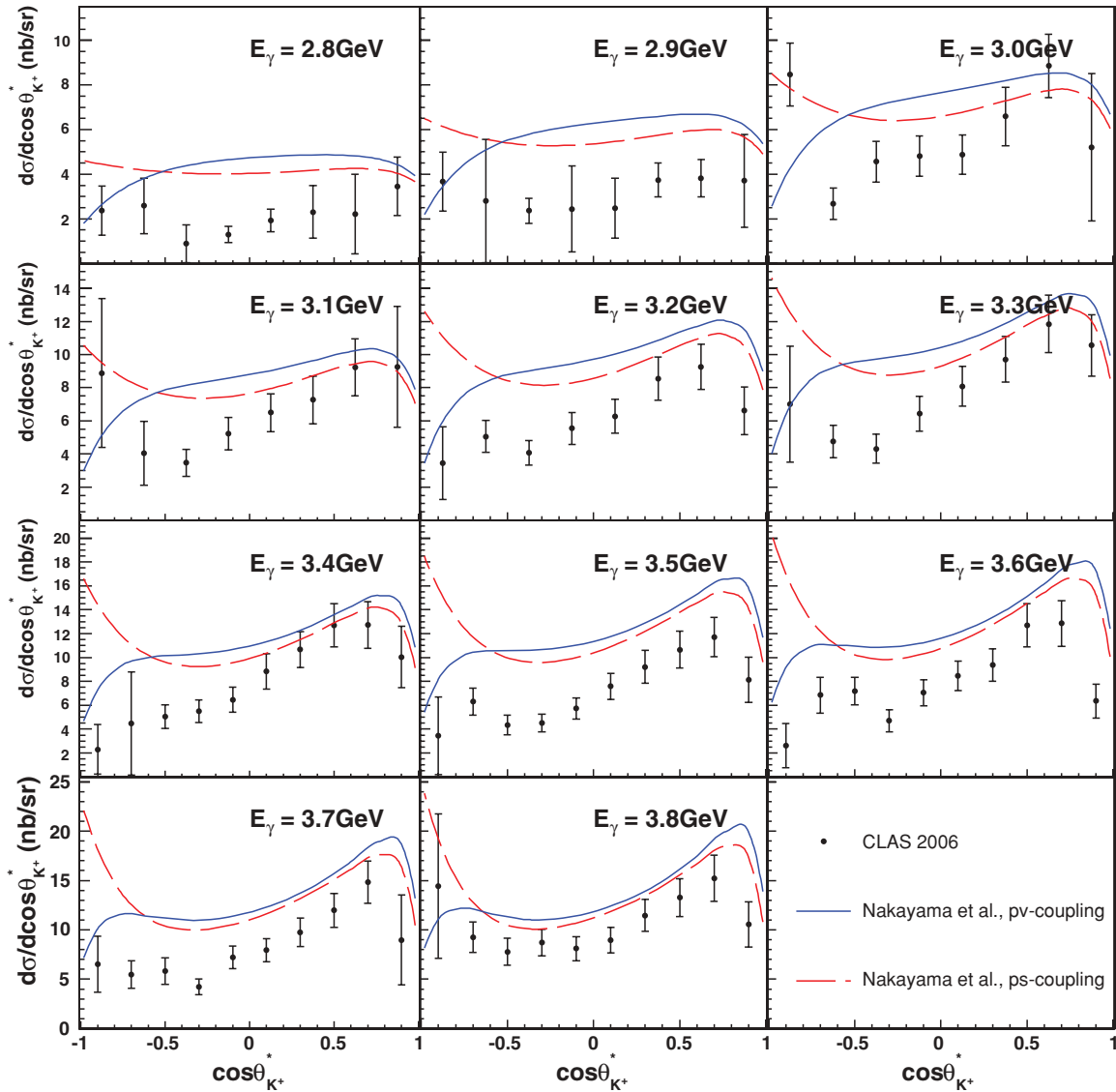


FIG. 6. (Color online) Differential cross section ( $d\sigma/d\cos\theta_{K^+}^*$ ) results (including both statistical and systematic uncertainties) from the current work compared with model predictions from Ref. [14]. The solid curves correspond to the predictions with the pv-coupling choice; the dashed curves correspond to the ps-coupling choice.

ranges such as the most forward or most backward regions of the detectors.

After the differential cross sections for the  $\Xi^-$  were obtained, the total cross sections (Fig. 7) were determined as a function of  $E_\gamma$  by integrating the differential cross sections. An additional systematic uncertainty, around 10%, as a result of the integration is extracted by comparing the results of integrating the four different sets of differential cross sections. The  $\Xi^-$  total cross section is determined to be around 2 nb at  $E_\gamma = 2.8$  GeV and rises to about 11 nb at 3.8 GeV. The rising cross section with  $E_\gamma$  is consistent with our conjecture for the simulation since higher photon energies simply provide more phase space, making it possible to produce other hyperon states that may decay to  $K^+\Xi^-$ .

For  $E_\gamma > 3.85$  GeV, the statistics are limited and it is not feasible to fine-tune the simulation model to match the data in terms of various differential cross sections. Instead,

the production of  $\Xi^-$  is assumed to be of the same origin as that at  $E_\gamma = 3.8$  GeV. The total-cross-section results are then extracted in six energy bins for the  $E_\gamma = 3.85\text{--}4.75$  GeV region. Larger systematic uncertainties, estimated to be around 20%, are included for the total-cross-section results above 3.85 GeV. Within uncertainties, the results are consistent with the continuation of the rise of  $\sigma(E_\gamma)$ , which is slightly different from the flattening behavior predicted in Ref. [14]. However, it should be pointed out that Ref. [14] used earlier preliminary results reported in Ref. [20], and it is likely the agreement between our data and the model could become significantly better.

It should be mentioned that the current results are higher than that reported earlier by CLAS ( $3.5 \pm 1.1$  nb for  $E_\gamma = 3.0\text{--}3.9$  GeV, [10]), which were obtained from data with much lower statistics. The difference at the same energy range is  $3.5 \pm 1.6$  nb, about two standard deviations from zero. This



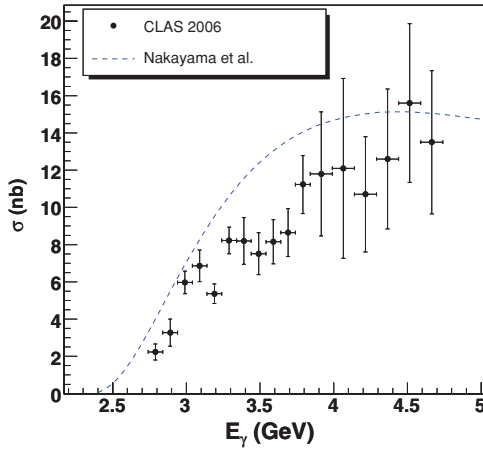


FIG. 7. (Color online) Total cross section of  $\Xi^-$  results (including both statistical and systematic uncertainties) from the current work compared with model predictions from Ref. [14].

difference is mainly due to the different model for the CLAS acceptance and underestimated systematics of the previous measurement.

#### IV. $\Xi^-(1530)$ RESULTS

The 700 events in the  $MM(K^+K^+)$  spectrum (Fig. 2) represent the highest statistics collected in exclusive photoproduction of the  $\Xi(1530)$  to date. The  $\Xi^-(1530)$  mass is found to be  $1537.8 \pm 0.9 \pm 2.4$  MeV/ $c^2$ , and the width is  $15.0 \pm 5.0$  MeV/ $c^2$ , both consistent with the previous measurements [2]. In the energy range of 3.35–4.75 GeV, the  $\Xi^-(1530)$  yields are extracted in eight  $\cos\theta_{\Xi^-(1530)}^*$  bins in the c.m. frame to obtain the differential cross section, shown in Fig. 8. [There is no  $\Xi^-(1530)$  signal below 3.35 GeV, owing to the low acceptance and production rate.] However, the statistics are not high enough to allow detailed model tuning for the simulation, which assumes a  $t$ -channel process that produces a hypothetical hyperon  $Y^*$  [ $M =$

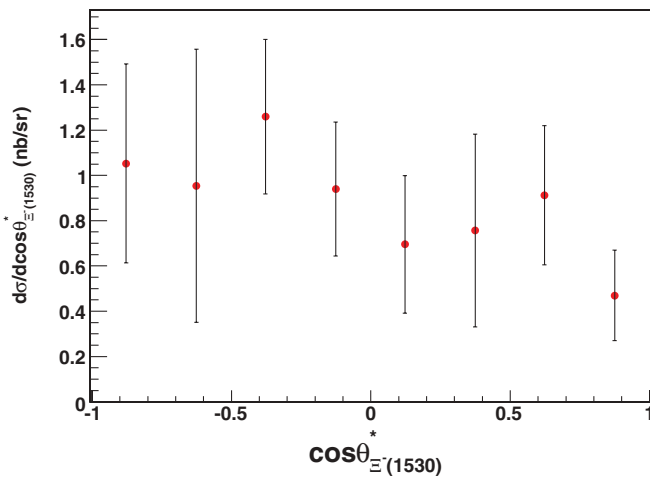


FIG. 8. (Color online) Differential cross sections for the  $\Xi^-(1530)$  in the photon energy range of 3.35–4.75 GeV. Both statistical and systematic uncertainties are included.

$2.155$  GeV/ $c^2$ ,  $\Gamma = 160$  MeV/ $c^2$ ,  $t$  slope =  $1.6$  (GeV/ $c^2$ ) $^{-2}$ ) production that decays to  $\Xi^-(1530)K^+$ . The systematic uncertainty resulting from the model dependence of the CLAS acceptance is estimated to be around 20%. The total cross section is then obtained by summing the differential cross section results and is  $1.76 \pm 0.24 \pm 0.13$  nb for  $E_\gamma = 3.35$ –4.75 GeV, less than 20% of that of the ground state in the comparable energy range.

To search for the excited cascade resonances, the reaction  $\gamma p \rightarrow K^+K^+\pi^-[\Xi^0]$  has been studied. The main contributing background process is  $\Xi^-$  production because of the consequent decays  $\Xi^- \rightarrow \Lambda\pi^-$ , and the missing particle from the  $K^+K^+\pi^-$  system would be the  $\Lambda$  (Fig. 9, top right). It is interesting to note that the  $\Xi^-$  signal reconstructed from the  $\Lambda\pi^-$  invariant mass (Fig. 9, bottom right) has a much better resolution ( $\sigma \sim 3$  MeV/ $c^2$ ) than that obtained using the missing mass technique (Fig. 2,  $\sigma \sim 7$  MeV/ $c^2$ ). The  $\Xi^-$  mass, as determined by the  $\Lambda\pi^-$  invariant mass, is  $1.3224$  GeV/ $c^2$ , consistent with that identified from the reaction  $\gamma p \rightarrow K^+K^+(X)$  via missing mass. However, the statistics are much lower owing to the low acceptance for the negative pion (around 10%). Therefore the  $\Xi^-$  cross-section results were extracted only by using the  $\gamma p \rightarrow K^+K^+(X)$  reaction. In addition, events with the  $\pi^-$  coming from  $\Lambda$  decay remain part of the background. To suppress this background, the vertex position from the  $\pi^-$  is required to be within the target area because of the weak decay of the  $\Lambda$ . If an additional proton is detected and the  $p\pi^-$  invariant mass falls close to the  $\Lambda$  region, the event is removed from the final data sample.

The  $K^+K^+\pi^-$  events with an additional  $\pi^+$  detected (about 20% of the total  $K^+K^+\pi^-$  events) are used to estimate the background, which is typically associated with those events where a  $\pi^+$  or proton is misidentified as a  $K^+$ . [Reactions such as  $\gamma p \rightarrow K^+\Lambda(1520)$ ,  $\Lambda(1520) \rightarrow \Lambda\pi\pi/\Sigma\pi$  can all contribute to this background.] This empirical background peaks around  $1.2$  GeV/ $c^2$  in the  $K^+K^+\pi^-$  missing mass spectrum, slightly overestimates the right shoulder of the  $\Lambda$  peak, and in general describes the data well near the  $\Xi^0$  peak (Fig. 9, left). The non- $\Xi^0$  event background is also explored by investigating those events originating from outside of the target, which are less likely to be associated with the  $\Xi^*$  production. The results are qualitatively the same.

Finally, about 270  $\Xi^0$  events can be identified from the  $K^+K^+\pi^-$  missing-mass spectrum in addition to the dominant  $\Lambda$  signal (Fig. 9, left). The  $\Xi^0$  events are then kinematically fitted by using the nominal  $\Xi^0$  mass of  $1.3148$  GeV/ $c^2$ . The final  $M(\Xi^0\pi^-)$  spectrum is shown in Fig. 10, where the  $\Xi^-(1530)$  is visible. For those events that are associated with non- $\Xi^0$ -production, events with low confidence level ( $CL < 10\%$ ) are used to study the background. The background obtained is included in the fit so that the total number of non- $\Xi^0$  events are within 10% of the expected number of events. Using other methods to estimate this background as discussed earlier, and also side-band events, yields similar results.

However, it should be pointed out that reactions such as  $\gamma p \rightarrow K^+K^*\Xi^0$ ,  $K^* \rightarrow K^+\pi^-$  and  $\gamma p \rightarrow K^+Y^*$ ,  $Y^* \rightarrow Y^*\pi^- \rightarrow K^+\pi^-\Xi^0$  may also contribute, complicating the interpretation of the spectrum. Knowledge of these processes is very limited, mostly because of the lack of data. The

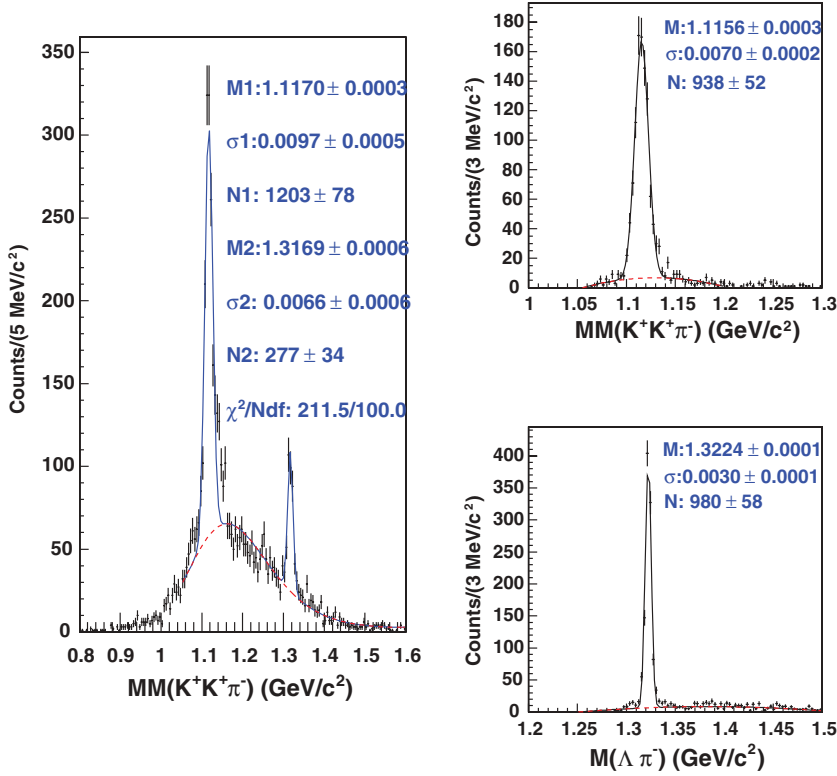


FIG. 9. (Color online) (Left)  $(K^+K^+\pi^-)$  missing mass spectrum. The dashed background shape is obtained from events with an additional  $\pi^+$  in the same event. (Top right)  $(K^+K^+\pi^-)$  missing mass with a  $3\sigma$  cut on the  $\Xi^-$  region [in the  $(K^+K^+)$  missing mass]. (Bottom right)  $(\Lambda\pi^-)$  invariant mass with a  $3\sigma$  cut on the  $\Lambda$  region [in the  $(K^+K^+\pi^-)$  missing mass]. Fitting parameter notation is the same as in Fig. 2.

first process is simulated with a  $t$ -channel process of  $K^*$  production with a heavy hyperon that decays to  $K^+\Xi^0$ , producing a background spectrum in the  $\Xi^0\pi^-$  invariant mass, as shown in the dot-dashed line of Fig. 10. The spectrum was fitted with a p-wave Breit-Wigner function atop the non- $\Xi^0$ -event background and the  $K^{*0}$  background, yielding about 70  $\Xi^-(1530)$  events (integrated from 1.50 to 1.8  $\text{GeV}/c^2$ ). The small enhancement around the 1.6  $\text{GeV}/c^2$  region has

a significance of less than 2.5 standard deviations and will be further discussed in the next section.

The cross section of the  $\Xi^-(1530)$  state can then be extracted and compared with the results obtained from the reaction  $\gamma p \rightarrow K^+K^+(X)$  discussed earlier. As a consistency check, by assuming a branching ratio of  $\frac{BR(\Xi^* \rightarrow \Xi^0\pi^-)}{BR(\Xi^* \rightarrow (\Xi\pi)^-)} = \frac{2}{3}$ , the  $\Xi^-(1530) \rightarrow (\Xi\pi)^-$  cross section for the energy range of 3.35–4.75 GeV has been determined to be  $1.60 \pm 0.41 \pm 0.21$  nb for the  $\Xi^-(1530)$ , obtained from differential cross sections extracted in four angular bins of the  $\Xi^0\pi^-$  system in the photon-proton c.m. frame. Within uncertainties, the branching ratio of the  $\Xi\pi$  channel of the  $\Xi^-(1530)$  decay extracted from these data,  $0.91 \pm 0.30$ , is consistent with the known value of 100%.

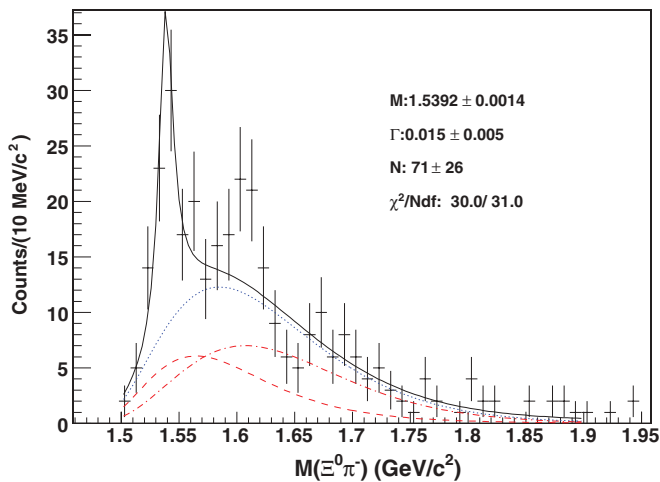


FIG. 10. (Color online)  $(\Xi^0\pi^-)$  invariant mass spectrum from events with  $CL > 0.1$ . The dashed line is the non- $\Xi^0$  background obtained from events with  $CL < 0.1$ , and the dash-dotted line is the  $K^{*0}$  background defined by  $\gamma p \rightarrow K^+K^{*0}\Xi^0$  simulation. The dotted line is the total background as the sum of these two backgrounds. The  $\Xi^-(1530)$  signal is parametrized by a p-wave Breit-Wigner function.

## V. $\Xi^0$ MASS AND THE $\Xi$ DOUBLET MASS SPLITTING

The mass of the  $\Xi^0$ , identified from the reaction  $\gamma p \rightarrow K^+K^+\pi^-[\Xi^0]$ , is measured to be  $1316.9 \pm 0.6 \pm 1.2$   $\text{MeV}/c^2$ , which is higher than the PDG value of  $1314.83 \pm 0.2$   $\text{MeV}/c^2$  [2]. The systematic uncertainty of 1.2  $\text{MeV}/c^2$  is derived from the dependence on the kinematic variables such as the  $\Xi^0$  laboratory angles. The  $\Xi$  doublet mass splitting can then be derived to be  $5.4 \pm 1.8$   $\text{MeV}/c^2$ , consistent with the PDG value of  $6.48 \pm 0.24$   $\text{MeV}/c^2$ . If the decay products of the  $\Xi^0$  are detected, the mass can be determined from invariant mass instead of missing mass, and this may lead to a better measurement of the  $\Xi$  doublet mass splitting. However, it is impossible to achieve with the current statistics.

VI. DISCUSSIONS OF  $\Xi^*$ 

Among the lighter cascade resonances, the  $\Xi(1620)$  is a controversial state that has only been reported in the  $\Xi\pi$  channel, with very limited statistics; it is assigned only one star in the most recent PDG [2]. The reported mass, between 1600 and 1630 MeV/ $c^2$ , seems to be too low for the second excited cascade resonance according to the constituent quark model [23]. Earlier evidence [24–26] has poor statistics. On the theoretical side, some dynamic models [27,28] have predicted a possible cascade resonance in the region of 1600 MeV/ $c^2$ . In the framework of a unitary extension of chiral perturbation theory [27], the  $\Xi(1620)$  emerged in the  $\Xi\pi$  invariant mass with a width around 50 MeV/ $c^2$ , and it is assigned to an octet together with the  $N^*(1535)$ , the  $\Lambda(1670)$ , and the  $\Sigma(1620)$ . These models clearly contradict the constituent quark model [23]. As for the  $\Xi(1690)$ , although it has recently been reported in the  $\Xi\pi$  channel [29], it has mostly been observed in the  $\Lambda/\Sigma K^-$  decay, which has very low acceptance in the current experiment.

In the two reactions reported here, there is no substantial signal for any excited cascade state beyond the  $\Xi^-(1530)$ . In the reaction  $\gamma p \rightarrow K^+ K^+(X)$ , although the presence of the  $\Xi^-(1530)$  is indubitable in the spectrum (Fig. 2), the data are consistent with background fluctuations in the  $\Xi^-(1620)$  and the  $\Xi^-(1690)$  regions. However, the absence of signals does not rule out the existence of these resonances, since it is likely that their production rate is too low to be observed owing to the low photon energies and limited acceptance in our experiment. For the reaction  $\gamma p \rightarrow K^+ K^+ \pi^- [\Xi^0]$ , the number of  $\Xi^-(1530)$  events is consistent with the expectation when compared with the reaction  $\gamma p \rightarrow K^+ K^+ [\Xi^-(1530)]$ . In Fig. 10, only the  $\Xi^-(1530)$  signal is of statistical significance. In fact, the simulated  $K^{*0}$  events also peak in the 1600 MeV/ $c^2$  region, where the largest fluctuation occurs. Limited by the low statistics, the interference effect is challenging to quantify, making the interpretation of the data more difficult. It is also worth reminding the reader that processes such as the reaction  $\gamma p \rightarrow K^+ Y^*$ ,  $Y^* \rightarrow Y^+ \pi^- \rightarrow K^+ \pi^- \Xi^0$  are not included in the background simulation. To perform a full partial-wave analysis and make more definite statements, an experiment with higher statistics is required.

## VII. SUMMARY

The  $\Xi$  doublet mass splitting is measured to be  $5.4 \pm 1.8$  MeV/ $c^2$ , consistent with the current global value of  $6.48 \pm 0.24$  MeV/ $c^2$ . In addition, the first detailed measurements of the  $\Xi^-$  photoproduction cross sections have been obtained from the reaction  $\gamma p \rightarrow K^+ K^+ [\Xi^-]$ . The  $\Xi^-$  angular distributions and  $K^+ \Xi^-$  invariant mass spectra are consistent with a production mechanism of  $Y^* \rightarrow \Xi^- K^+$  through a  $t$ -channel process. However, the current analysis is not sufficient to draw definite conclusions in terms of the production mechanism nor to determine the quantum numbers of the intermediate hyperon resonances. The differential photoproduction cross sections of the  $\Xi^-(1530)$  have also been measured for the first time through the reaction  $\gamma p \rightarrow K^+ K^+(X)$ , and the  $\Xi^-(1530)$  is also observed in the reaction  $\gamma p \rightarrow K^+ K^+ \pi^- [\Xi^0]$  as well. Although a small enhancement is observed in the  $\Xi^0 \pi^-$  invariant mass spectrum near the controversial one-star  $\Xi^-(1620)$  resonance, it is not possible to determine its exact nature without a full partial-wave analysis, because of the very limited statistics. This limitation will be addressed by a future, higher energy photon experiment using a hydrogen target that is currently planned in CLAS at Jefferson Laboratory [30].

## ACKNOWLEDGMENTS

We would like to acknowledge the outstanding efforts of the JLab Accelerator and the Physics Division staff, and especially the g11 running group, who made this experiment possible. We would like to thank B. Nefkens and S. Capstick for useful discussions. This work was supported in part by the U.S. Department of Energy, the National Science Foundation, the Istituto Nazionale di Fisica Nucleare, the French Centre National de la Recherche Scientifique, the French Commissariat à l’Energie Atomique, an Emmy Noether grant from the Deutsche Forschungs Gemeinschaft, the Research Corporation, and the Korean Science and Engineering Foundation. Jefferson Science Associates (JSA) operates the Thomas Jefferson National Accelerator Facility for the United States Department of Energy under Contract No. DE-AC05-06OR23177.

- 
- [1] B. M. K. Nefkens, presented at Workshop on 50-GeV Japanese Hadron Facility (1995).
  - [2] W. M. Yao *et al.*, *J. Phys. G* **33**, 1 (2006).
  - [3] A. Duncan, E. Eichten, and H. Thacker, *Nucl. Phys. Proc. Suppl.* **53**, 299 (1997).
  - [4] R. Delbourgo, D. Liu, and M. Scadron, *Phys. Rev. D* **59**, 113006 (1999).
  - [5] V. Fanti *et al.*, *Eur. Phys. J. C* **12**, 69 (2000).
  - [6] R. A. Muller, Ph.D. thesis UCRL 19372 (1968).
  - [7] G. Burgun *et al.*, *Nucl. Phys.* **B8**, 447 (1968).
  - [8] R. D. Tripp *et al.*, *Nucl. Phys.* **B3**, 10 (1967).
  - [9] P. J. Litchfield *et al.*, *Nucl. Phys.* **B30**, 125 (1971).
  - [10] J. W. Price *et al.*, *Phys. Rev. C* **71**, 058201 (2005).
  - [11] D. Aston *et al.*, *Nucl. Phys.* **B198**, 189 (1982).
  - [12] K. Abe *et al.*, *Phys. Rev. D* **32**, 2869 (1985).
  - [13] A. Donnachie, *Z. Phys. C* **4**, 161 (1980).
  - [14] K. Nakayama, Y. Oh, and H. Haberzettl, *Phys. Rev. C* **74**, 035205 (2006).
  - [15] B. A. Mecking *et al.*, *Nucl. Instrum. Methods A* **503**, 513 (2003).
  - [16] D. Sober *et al.*, *Nucl. Instrum. Methods A* **440**, 263 (2000).
  - [17] M. D. Mestayer *et al.*, *Nucl. Instrum. Methods A* **449**, 81 (2000).
  - [18] E. S. Smith *et al.*, *Nucl. Instrum. Methods A* **432**, 265 (1999).
  - [19] Y. G. Sharabian *et al.*, *Nucl. Instrum. Methods A* **556**, 246 (2006).
  - [20] L. Guo and D. P. Weygand (CLAS Collaboration), in *Proceedings of the International Workshop on the Physics of Excited Baryons (NSTAR’05), Tallahassee, Florida, October 2005*, edited by S. Capstick, V. Crede, and P. Eugenio (World Scientific, Singapore, 2006), p. 384.
  - [21] S. Stepanyan *et al.*, *Nucl. Instrum. Methods A* **572**, 654 (2007).

- [22] V. I. Mokeev *et al.*, in *Proceedings of the International Workshop on the Physics of Excited Baryons (NSTAR'05), Tallahassee, Florida, October 2005*, edited by S. Capstick, V. Crede, and P. Eugenio (World Scientific, Singapore, 2006), p. 47.
- [23] K. T. Chao, N. Isgur, and G. Karl, *Phys. Rev. D* **23**, 155 (1981).
- [24] E. Briefel *et al.*, *Phys. Rev. D* **16**, 2706 (1977).
- [25] A. de Bellefon *et al.*, *Nuovo Cim. A* **28**, 289 (1975).
- [26] R. T. Ross *et al.*, *Phys. Lett.* **B38**, 177 (1972).
- [27] A. Ramos, E. Oset, and C. Bennhold, *Phys. Rev. Lett.* **89**, 252001 (2002).
- [28] Y. I. Azimov, R. A. Arndt, I. I. Strakovsky, R. L. Workman, *Phys. Rev. C* **68**, 045204 (2003).
- [29] M. I. Adamovich *et al.*, *Eur. Phys. J. C* **5**, 621 (1998).
- [30] D. P. Weygand *et al.*, Jefferson Laboratory Proposal E-04-017, 2004.